

Article

# Optimization of Complex Function Expansions for Gauss-Krüger Projections

Xiaoyong Li <sup>1</sup> , Houpu Li <sup>1,\*</sup>, Guohui Liu <sup>2</sup> and Shaofeng Bian <sup>1</sup>

<sup>1</sup> College of Electrical Engineering, Naval University of Engineering, Wuhan 430033, China

<sup>2</sup> Chart Information Center, Tianjin 300450, China

\* Correspondence: 2018301020028@whu.edu.cn

**Abstract:** Compared with complex and lengthy Gauss-Krüger projection series expansions and real number expressions, we improve the complex function representation of Gauss-Krüger projections and rewrite them into the “multiple Angle form”, “exponential form”, and “double Angle form”. The coefficients were expanded in the power series based on the first eccentricity  $e$  and the third flattening  $n$ , respectively, and the truncation difference was analyzed when expanded to different orders to obtain the simplified practical formulas for each form on the premise of meeting the accuracy requirements of geodesy. Through numerical analysis, the computational efficiency of the forward and inverse solutions of the Gauss-Krüger projection is analyzed, which shows the superiority of the “double Angle form”. Through the above measures, the expressions for forward and inverse solutions of the Gauss-Krüger projection are obtained, meeting the accuracy requirements with a higher computational efficiency and a more concise form.

**Keywords:** map projection; complex function; truncation difference analysis; computer algebra system



**Citation:** Li, X.; Li, H.; Liu, G.; Bian, S. Optimization of Complex Function Expansions for Gauss-Krüger Projections. *ISPRS Int. J. Geo-Inf.* **2022**, *11*, 566. <https://doi.org/10.3390/ijgi11110566>

Academic Editors: Florian Hruby and Wolfgang Kainz

Received: 19 September 2022

Accepted: 5 November 2022

Published: 11 November 2022

**Publisher’s Note:** MDPI stays neutral with regard to jurisdictional claims in published maps and institutional affiliations.



**Copyright:** © 2022 by the authors. Licensee MDPI, Basel, Switzerland. This article is an open access article distributed under the terms and conditions of the Creative Commons Attribution (CC BY) license (<https://creativecommons.org/licenses/by/4.0/>).

## 1. Introduction

Navigation is inseparable from maps; without high-precision maps as information carriers, a navigation system is only a positioning system [1–3]. In particular, the trend of electronic and intelligent development of maps and charts also puts forward higher requirements on the efficiency and accuracy of projections’ forward and inverse solution formulas [4–7]. The Gauss-Krüger projection is one of the most important conformal projections and is widely used in geodesy, cartography, engineering surveying, and other fields [8]. It has unique advantages in land–sea transition map and large-scale map construction. At present, this projection is used as the mathematical basis of topographic maps of the world and many countries. [9].

Gauss-Krüger projection theory has long been studied by scholars and has made new progress in modern research. Abbey et al. discussed the application of the oblique Mercator projection in modern engineering surveys and demonstrated its superiority through calculations [10]. Sergio derived direct and transverse Mercator-type projections for the constant-height surface-to-plane conformal mapping, and the precision of the formula was analyzed by numerical analysis [11]. However, due to the limitation of historical conditions, many mathematical analysis processes were completed manually at that time, and the order and accuracy of the expansion formulas could not be very high; sometimes, there were small mistakes that were not easy to find, especially since the inverse solution was often presented as an iterative form that was not suitable for mathematical analysis [12]. So, it is necessary to use an advanced computer algebraic analysis to make necessary improvements and innovations.

Because of the connection between the theory of complex functions and conformal projections, it is often useful to represent coordinates with complex numbers when working with conformal mappings [13,14]. The theory of complex functions’ representation of

map projections is as old as complex analysis is. Many scholars have made very meaningful works in this field. Bowring discussed the complex function representation of the Gauss-Krüger projection [15]. Klotz gave the Gauss-Krüger projection a complex function solution for arbitrary bandwidth based on an effective recursive formula [16]. Schuhr gave the Fortran program of forward and backward solutions of the Gauss-Krüger projection expressed by complex functions according to the formula in [16] and calculated them [17]. With the help of a computer algebra system, the forward and inverse solution formulas of the Gauss-Krüger projection complex function expression are calculated by iterative solutions, and the scale ratio and meridian convergence angle of the complex function expression are derived [18–20]. All these show the superiority of applying complex functions to solve the mathematical problem of the Gauss-Krüger projection. Guo Jiachun realized the non-iterative process of forward and inverse solutions of the Gauss-Krüger projection based on Lee’s formula and revealed the essential process of the Gauss-Krüger projection [21,22]. Karney described two algorithms for the transverse Mercator projection, one of which is based on Thompson and Lee’s more accurate formulation and achieves an accuracy of 9 nanometers across the entire ellipsoid, and the other algorithm is a series expansion method. Because the Gauss-Krüger projection cannot be expressed in terms of elementary functions, the mapping is usually computed by means of a truncated series. Karney took Krüger’s research further and expanded the original series to  $n^{30}$ , which led to the new transverse Mercator algorithm with an accuracy of a few nanometers within a certain range [23,24]. However, although the high-order expansion achieves extremely high accuracy, it also makes the series expansion rather long and complex, which makes the formula difficult to propagate and the computational efficiency is low.

In this paper, the expression of complex functions of the Gauss-Krüger projection is studied by means of series expansion. The symbolic expressions of forward and inverse solutions without iteration are derived. We improve and modify the traditional forward and inverse solutions of the Gauss-Krüger projection of ellipsoids and rewrite them into the complex function expressions expressed in “multiple Angle form”, “exponential form”, and “double Angle form”. Based on the first eccentricity  $e$  and the third flattening  $n$ , the coefficients in the formulas are expanded in power series, respectively, and the truncation difference of the coefficients expanded to different orders is analyzed to obtain the simplified practical formulas of each form on the premise of meeting the accuracy requirements of geodesy. Through numerical analysis, the computational efficiency of the forward and inverse solutions of the Gauss-Krüger projection is analyzed and the forward and inverse solution algorithm of the Gauss-Krüger projection with the highest computational efficiency is obtained.

## 2. Complex Function Expression of the Gauss-Krüger Projection

According to the literature [25,26], in the Gauss-Krüger projection plane,  $x$  is the ordinate, which is the northbound coordinate; and  $y$  represents the abscissa, that is, the east coordinate. In addition,  $l$  represents the longitude difference,  $B$  represents geodetic latitude,  $X(B) = a(1 - e^2) \int_0^B \frac{dB}{\sqrt{(1 - e^2 \sin^2 B)^{3/2}}}$ ,  $N = \frac{a}{\sqrt{1 - e^2 \sin^2 B}}$ ,  $t = \tan B$ , and  $\eta^2 = e'^2 \cos^2 B$ . In the inverse solution, the base point latitude  $B_f$  needs to be solved iteratively. Then, the traditional Gauss-Krüger projection real number expression is:

$$\begin{cases} x = X + Nt \cos^2 B \frac{l^2}{\rho^2} \left[ 0.5 + \frac{1}{24}(5 - t^2 + 9\eta^2 + 4\eta^4) \cos^2 B \frac{l^2}{\rho^2} + \frac{1}{720}(61 - 58t^2 + t^4) \cos^4 B \frac{l^4}{\rho^4} \right] \\ y = N \cos B \frac{l}{\rho} \left[ 1 + \frac{1}{6}(1 - t^2 + \eta^2) \cos^2 B \frac{l^2}{\rho^2} + \frac{1}{120}(5 - 18t^2 + t^4 + 14\eta^2 - 58t^2\eta^2) \cos^4 B \frac{l^4}{\rho^4} \right] \\ B = B_f - \frac{\rho t_f}{2M_f} y \left( \frac{y}{N_f} \right) \left[ 1 - \frac{1}{12}(5 + 3t_f^2 + \eta_f^2 - 9\eta_f^2 t_f^2) \left( \frac{y}{N_f} \right)^2 + \frac{1}{360M_f N_f^5} (61 + 90t_f^2 + 45t_f^4) \left( \frac{y}{N_f} \right)^4 \right] \\ l = \frac{\rho}{\cos B_f} \left( \frac{y}{N_f} \right) \left[ 1 - \frac{1}{6}(1 + 2t_f^2 + \eta_f^2) \left( \frac{y}{N_f} \right)^2 + \frac{1}{120}(5 + 28t_f^2 + 24t_f^4 + 6\eta_f^2 + 8\eta_f^4 t_f^2) \left( \frac{y}{N_f} \right)^4 \right] \end{cases} \quad (1)$$

In practical calculation, Equation (1) is often expressed as the power series of longitude difference  $l$ . In order to reduce the deformation in the east–west direction, it is often necessary to divide it into  $3^\circ$  or  $6^\circ$  zones. The zoning map can be drawn by using the mathematical relationship of Equation (1), as shown in Figure 1.

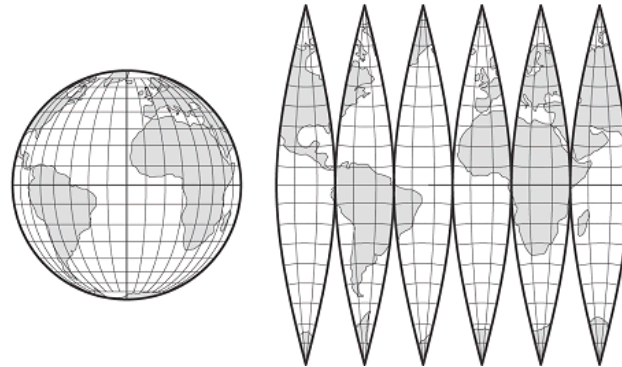


Figure 1. Sketch of Gauss-Krüger projection.

Although zoning increases the usability of Gauss-Krüger projection in east–west direction, it also creates a lack of continuity, especially in polar maps, which are fragmented and cannot be applied. In view of the natural relationship between complex functions and conformal mapping, some scholars have introduced this mathematical method into the study of conformal projection in recent years. Bian Shaofeng extended the forward and inverse solutions of the meridian arc length from the real number field to the complex number field through iterative mathematical methods, and gave the complex variable function formula of the Gauss-Krüger projection [15,27]:

$$\begin{cases} q = \operatorname{arctanh}(\sin B) - e \cdot \operatorname{arctanh}(e \sin B) \\ \mathbf{w} = q + i l = \operatorname{arctanh}(\sin B) - e \cdot \operatorname{arctanh}(e \sin B) + i l \\ \varphi = \arcsin[\tanh(\mathbf{w})] \\ z = x + iy = a(a_0 \varphi + a_2 \sin 2\varphi + a_4 \sin 4\varphi + a_6 \sin 6\varphi + a_8 \sin 8\varphi + a_{10} \sin 10\varphi) \end{cases} \quad (2)$$

In Formula (2),  $\mathbf{w} = q + il$  is the expression for isometric latitude in the field of complex functions, where  $q$  is isometric latitude, which is the expression of geodetic latitude  $B$ ,  $l$  is longitude difference, and  $a_i$  is the constant coefficient expressed by the first eccentricity  $e$ . The Gauss-Krüger projection expansion represented by the complex function is the power series form of the first eccentricity  $e$  of the ellipsoid, which has the advantages of fast convergence and not needing to divide.

However, for the polar region, when the geodetic latitude  $B$  approaches  $90^\circ$ , the isometric latitude  $q$  approaches infinity, which causes some trouble to the forward and inverse solutions of the Gauss-Krüger projection in the polar region. In order to solve this problem, the conformal co-latitude  $\theta = \frac{\pi}{2} - \varphi$  is introduced, where  $\varphi$  is the conformal latitude,

$\varphi = 2\arctan\sqrt{\frac{1+\sin B}{1-\sin B} \left(\frac{1-e \sin B}{1+e \sin B}\right)^e} - \frac{\pi}{2}$ , then the conformal co-latitude can be expressed as:

$$\begin{aligned} \theta &= \pi - 2\arctan\sqrt{\frac{1+\sin B}{1-\sin B} \left(\frac{1-e \sin B}{1+e \sin B}\right)^e} = 2\left(\frac{\pi}{2} - \arctan(\exp(q))\right) \\ &= 2\arctan(\exp(-q)) = 2\arctan\sqrt{\frac{1-\sin B}{1+\sin B} \left(\frac{1+e \sin B}{1-e \sin B}\right)^e} \end{aligned} \quad (3)$$

The change curve of the isometric latitude  $q$  and conformal co-latitude  $\theta$  with geodetic latitude  $B$  is shown in Figures 2 and 3.

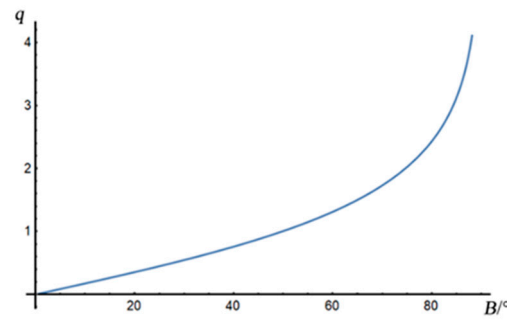


Figure 2. Sketch of isometric latitude  $q$  with geodetic latitude  $B$ .

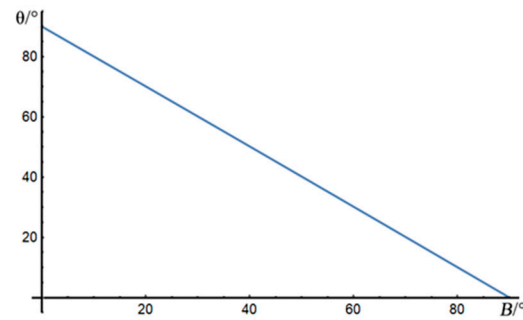


Figure 3. Sketch of conformal co-latitude  $\theta$  with geodetic latitude  $B$ .

According to Equation (3) and Figure 3, when  $0^\circ \leq B \leq 90^\circ$ ,  $\theta$  is always available. By substituting  $\theta$  into Equation (2), the expression of the forward solution of the Gauss-Krüger projection complex function can be obtained:

$$\begin{cases} q = \operatorname{arctanh}(\sin B) - e \cdot \operatorname{arctanh}(e \sin B) \\ \mathbf{w} = q + i l = \operatorname{arctanh}(\sin B) - e \cdot \operatorname{arctanh}(e \sin B) + i l \\ \theta = 2\operatorname{arctan}[\exp(-\mathbf{w})] \\ z = x + iy = a(\alpha_0\theta - \alpha_2 \sin 2\theta + \alpha_4 \sin 4\theta - \alpha_6 \sin 6\theta + \alpha_8 \sin 8\theta - \alpha_{10} \sin 10\theta) \end{cases} \quad (4)$$

According to the literature [26], the relationship between the third flattening  $n$  and the first eccentricity  $e$  of the ellipsoid is:

$$n = \frac{a - b}{a + b} = \frac{1 - \sqrt{1 - e^2}}{1 + \sqrt{1 - e^2}} \quad (5)$$

with the help of the computer algebra system; the coefficients in Equation (4) are expanded in terms of  $e$  up to  $e^{10}$  and in terms of  $n$  up to  $n^5$ , which is shown in Table 1:

Table 1. Coefficients in Equation (4).

Coefficient Representation Based on $e$	Coefficient Representation Based on $n$
$\begin{cases} a_0 = 1 - \frac{e^2}{4} - \frac{3e^4}{64} - \frac{5e^6}{256} - \frac{175e^8}{16384} - \frac{441e^{10}}{65536} \\ a_2 = \frac{e^2}{8} - \frac{e^4}{96} - \frac{9e^6}{1024} - \frac{901e^8}{184320} - \frac{16381e^{10}}{5898240} \\ a_4 = \frac{13e^4}{768} + \frac{17e^6}{5120} - \frac{311e^8}{737280} - \frac{18931e^{10}}{20643840} \\ a_6 = \frac{61e^6}{15360} + \frac{899e^8}{430080} + \frac{14977e^{10}}{27525120} \\ a_8 = \frac{49561e^8}{41287680} + \frac{175087e^{10}}{165150720} \\ a_{10} = \frac{34729e^{10}}{82575360} \end{cases}$	$\begin{cases} \alpha_0 = 1 - n + \frac{5}{4}n^2 - \frac{5}{4}n^3 + \frac{81}{64}n^4 - \frac{81}{64}n^5 \\ \alpha_2 = \frac{1}{2}n - \frac{7}{6}n^2 + \frac{77}{48}n^3 - \frac{1111}{720}n^4 + \frac{2281}{1920}n^5 \\ \alpha_4 = \frac{13}{48}n^2 - \frac{209}{240}n^3 + \frac{3817}{2880}n^4 - \frac{6917}{6720}n^5 \\ \alpha_6 = \frac{61}{240}n^3 - \frac{1663}{1680}n^4 + \frac{14459}{8960}n^5 \\ \alpha_8 = \frac{49561}{161280}n^4 - \frac{221401}{161280}n^5 \\ \alpha_{10} = \frac{34729}{80640}n^5 \end{cases}$

It can be found that when the coefficients in Formula (4) are expanded in a power series based on the third flattening  $n$ , the form is more neat and more compact and the coefficients are simpler, which simplifies the formula to some extent and improves the calculation

efficiency. Co-latitude  $\theta$  and complex functions are introduced so that Equation (4) can also be applied in the polar region.

According to the literature [24,25], the inverse solution formula of the Gauss-Krüger projection can be derived from Equation (4):

$$\begin{cases} \omega = \frac{z}{a\alpha_0} = \frac{x+iy}{a\alpha_0} \\ \theta = -\omega + b_2 \sin 2\omega + b_4 \sin 4\omega + b_6 \sin 6\omega + b_8 \sin 8\omega + b_{10} \sin 10\omega \end{cases} \quad (6)$$

Similarly, the coefficients in Equation (6) are expanded in terms of  $e$  up to  $e^{10}$  and in terms of  $n$  up to  $n^5$ , which is shown in Table 2:

Table 2. Coefficients in Equation (6).

Coefficient Representation Based on $e$	Coefficient Representation Based on $n$
$\begin{cases} b_2 = -\frac{e^2}{8} - \frac{e^4}{48} - \frac{47e^6}{2048} + \frac{17e^8}{184320} + \frac{17837e^{10}}{23592960} \\ b_4 = \frac{e^4}{768} + \frac{3e^6}{1280} + \frac{559e^8}{368640} + \frac{1021e^{10}}{1290240} \\ b_6 = -\frac{17e^6}{30720} - \frac{283e^8}{430080} - \frac{7489e^{10}}{13762560} \\ b_8 = -\frac{4397e^8}{41287680} + \frac{1319e^{10}}{6881280} \\ b_{10} = -\frac{4583e^{10}}{165150720} \end{cases}$	$\begin{cases} b_2 = -\frac{1}{2}n + \frac{2}{3}n^2 - \frac{157}{96}n^3 + \frac{2701}{360}n^4 - \frac{13359}{512}n^5 \\ b_4 = \frac{1}{48}n^2 + \frac{1}{15}n^3 - \frac{437n^4}{1440} + \frac{46}{105}n^5 \\ b_6 = -\frac{17}{480}n^3 + \frac{37}{840}n^4 + \frac{209}{4480}n^5 \\ b_8 = -\frac{4397}{161280}n^4 + \frac{4177}{10080}n^5 \\ b_{10} = -\frac{4583}{161280}n^5 \end{cases}$

After obtaining the complex conformal co-latitude  $\theta$ , according to its definition  $\theta = 2\arctan(\exp(-q + il))$ , the following Equation (7) can be obtained:

$$\begin{aligned} \tan \frac{\theta}{2} &= \exp(-q + il) = \exp(-q) \cos l - i \exp(-q) \sin l \\ \Rightarrow \theta &= 2\arctan \left| \tan \frac{\theta}{2} \right| \\ \Rightarrow \varphi &= \frac{\pi}{2} - \theta \end{aligned} \quad (7)$$

After the conformal latitude  $\varphi$  is calculated from Equation (7), the geodetic latitude  $B$  can be obtained according to [28]:

$$B = \varphi + m_2 \sin 2\varphi + m_4 \sin 4\varphi + m_6 \sin 6\varphi + m_8 \sin 8\varphi + m_{10} \sin 10\varphi \quad (8)$$

In Equation (8), the coefficients are shown in Table 3:

Table 3. Coefficients in Equation (8).

Coefficient Representation Based on $e$	Coefficient Representation Based on $n$
$\begin{cases} m_2 = \frac{1}{2}e^2 + \frac{5}{24}e^4 + \frac{1}{12}e^6 + \frac{13}{360}e^8 + \frac{3}{160}e^{10} \\ m_4 = \frac{7}{48}e^4 + \frac{29}{240}e^6 + \frac{811}{11520}e^8 + \frac{81}{2240}e^{10} \\ m_6 = \frac{120}{120}e^6 + \frac{81}{1120}e^8 + \frac{3029}{53760}e^{10} \\ m_8 = \frac{4279}{161280}e^8 + \frac{883}{20160}e^{10} \\ m_{10} = \frac{2087}{161280}e^{10} \end{cases}$	$\begin{cases} m_2 = 2n - \frac{2}{3}n^2 - 2n^3 + \frac{116}{45}n^4 + \frac{26}{45}n^5 \\ m_4 = \frac{7}{3}n^2 - \frac{8}{5}n^3 - \frac{227}{45}n^4 + \frac{2704}{315}n^5 \\ m_6 = \frac{36}{15}n^3 - \frac{136}{35}n^4 - \frac{1262}{105}n^5 \\ m_8 = \frac{4379}{630}n^4 - \frac{332}{35}n^5 \\ m_{10} = \frac{4174}{315}n^5 \end{cases}$

To sum up, Equations (4) and (6) solve the problems of the forward and inverse solutions of the Gauss-Krüger projection and avoid zoning. Compared with the above coefficients, it can be concluded that when the third flattening  $n$  replaces the first eccentricity  $e$ , the coefficients of each expression are smaller in value and more compact in form, which improves the efficiency of coordinate transformation to a certain extent.

### 3. Modification of the Complex Function Expression form of the Gauss-Krüger Projection

Practical cartographic work involves not only the coordinate transformation of points, but also the mapping of lines and surfaces. The process of map projection involves a huge number of calculations, which puts forward higher requirements for the calculation efficiency of the mathematical relations of the projection. In view of this, for the convenience of description, Equations (4) and (6) are respectively defined as the “multiple Angle form”

of the Gauss-Krüger projection complex function expression. This section will make modifications of them in order to obtain a more suitable form for computer calculation.

3.1. Form 1: "Power Exponential Form"

On the basis of Equation (4), the forward solution formula of the Gauss-Krüger projection complex function of "power exponential form" is derived as follows:

$$z = x + iy = ac_0\theta + a \cos \theta \left( c_1 \sin \theta + c_3 \sin^3 \theta + c_5 \sin^5 \theta + c_7 \sin^7 \theta + c_9 \sin^9 \theta \right) \quad (9)$$

According to Equation (4), the coefficients in Equation (9) are:

$$\begin{cases} c_0 = a_0 \\ c_1 = -2a_2 + 4a_4 - 6a_6 + 8a_8 - 10a_{10} \\ c_3 = -8a_4 + 32a_6 - 80a_8 + 160a_{10} \\ c_5 = -32a_6 + 192a_8 - 672a_{10} \\ c_7 = -128a_8 + 1024a_{10} \\ c_9 = -512a_{10} \end{cases} \quad (10)$$

Similarly, the coefficients in Equation (9) are expanded in terms of  $e$  up to  $e^{10}$  and in terms of  $n$  up to  $n^5$ , which is shown in Table 4

Table 4. Coefficients in Equation (9).

Coefficient Representation Based on $e$	Coefficient Representation Based on $n$
$\begin{cases} c_0 = a \left( 1 - \frac{1}{4}e^2 - \frac{3}{64}e^4 - \frac{5}{256}e^6 - \frac{175}{16384}e^8 - \frac{441}{65536}e^{10} \right) \\ c_1 = -\frac{1}{4}e^2 + \frac{17}{192}e^4 + \frac{9}{1280}e^6 + \frac{26581}{5160960}e^8 + \frac{19937}{6881280}e^{10} \\ c_3 = -\frac{13}{96}e^4 + \frac{193}{1920}e^6 - \frac{22163}{860160}e^8 + \frac{74593}{10321920}e^{10} \\ c_5 = -\frac{61}{480}e^6 + \frac{35177}{215040}e^8 - \frac{82993}{860160}e^{10} \\ c_7 = -\frac{49561}{322560}e^8 + \frac{126859}{430080}e^{10} \\ c_9 = -\frac{34729}{161280}e^{10} \end{cases}$	$\begin{cases} c_0 = 1 - n + \frac{5}{4}n^2 - \frac{5}{4}n^3 + \frac{81}{64}n^4 - \frac{81}{64}n^5 \\ c_1 = -n + \frac{41}{12}n^2 - \frac{493}{60}n^3 + \frac{338389}{20160}n^4 - \frac{126865}{4032}n^5 \\ c_3 = -\frac{13}{6}n^2 + \frac{151}{10}n^3 - \frac{224659}{3360}n^4 + \frac{2405113}{10080}n^5 \\ c_5 = -\frac{122}{15}n^3 + \frac{76169}{840}n^4 - \frac{507881}{840}n^5 \\ c_7 = -\frac{49561}{1260}n^4 + \frac{155413}{252}n^5 \\ c_9 = -\frac{34729}{315}n^5 \end{cases}$

After the calculation of  $z$ , other calculation processes are consistent with Equation (4) and will not be described here.

On the basis of Equation (6), the inverse solution formula of Gauss-Krüger projection complex function of "power exponential form" is derived as follows:

$$\theta = -\omega + \left( j_1 \sin \omega + j_3 \sin^3 \omega + j_5 \sin^5 \omega + j_7 \sin^7 \omega + j_9 \sin^9 \omega \right) \cos \omega \quad (11)$$

According to Equation (6), the coefficients in Equation (11) are:

$$\begin{cases} j_1 = 2b_2 + 4b_4 + 6b_6 + 8b_8 + 10b_{10} \\ j_3 = -8b_4 - 32b_6 - 80b_8 + 160b_{10} \\ j_5 = 32b_6 + 192b_8 + 672b_{10} \\ j_7 = -128b_8 - 1024b_{10} \\ j_9 = 512b_{10} \end{cases} \quad (12)$$

Similarly, the coefficients in Equation (11) are expanded in terms of  $e$  up to  $e^{10}$  and in terms of  $n$  up to  $n^5$ , which is shown in Table 5:

After the calculation of  $\theta$ , the other calculation processes are consistent with Equation (6) and will not be described here.

**Table 5.** Coefficients in Equation (11).

Coefficient Representation Based on $e$	Coefficient Representation Based on $n$
$\begin{cases} j_1 = -\frac{1}{4}e^2 - \frac{7}{192}e^4 - \frac{51}{1280}e^6 + \frac{1069}{737280}e^8 + \frac{11017}{4128768}e^{10} \\ j_3 = -\frac{1}{96}e^4 - \frac{1}{960}e^6 + \frac{6431}{368640}e^8 + \frac{971}{5160960}e^{10} \\ j_5 = -\frac{17}{960}e^6 - \frac{85}{2048}e^8 + \frac{85}{114688}e^{10} \\ j_7 = \frac{4397}{322560}e^8 + \frac{313}{80640}e^{10} \\ j_9 = -\frac{4583}{322560}e^{10} \end{cases}$	$\begin{cases} j_1 = -n + \frac{17}{12}n^2 - \frac{193}{60}n^3 + \frac{39853}{2880}n^4 - \frac{316649}{6720}n^5 \\ j_3 = -\frac{1}{6}n^2 + \frac{3}{5}n^3 + \frac{4607}{1440}n^4 - \frac{18817}{560}n^5 \\ j_5 = -\frac{17}{15}n^3 - \frac{153}{40}n^4 + \frac{34697}{560}n^5 \\ j_7 = \frac{4397}{1260}n^4 - \frac{838}{35}n^5 \\ j_9 = -\frac{4583}{315}n^5 \end{cases}$

3.2. Form 2: “Double Angle Form”

On the basis of Equation (4), the forward solution formula of the Gauss-Krüger projection complex function represented by “double Angle form” is derived as follows:

$$z = x + iy = ak_0\theta + a \sin 2\theta(k_1 + (k_2 + (k_3 + (k_4 + k_5 \cos 2\theta) \cos 2\theta) \cos 2\theta) \cos 2\theta) \quad (13)$$

According to Equation (4), the coefficients in Equation (13) are:

$$\begin{cases} k_0 = a_0 \\ k_1 = -a_2 + a_6 - a_{10} \\ k_2 = 2a_4 - 4a_8 \\ k_3 = -4a_6 + 12a_{10} \\ k_4 = 8a_8 \\ k_5 = -16a_{10} \end{cases} \quad (14)$$

Similarly, the coefficients in Equation (13) are expanded in terms of  $e$  up to  $e^{10}$  and in terms of  $n$  up to  $n^5$ , which is shown in Table 6:

**Table 6.** Coefficients in Equation (13).

Coefficient Representation Based on $e$	Coefficient Representation Based on $n$
$\begin{cases} k_0 = -\frac{1}{4}e^2 + \frac{17}{192}e^4 + \frac{9}{1280}e^6 + \frac{26581}{5160960}e^8 + \frac{19937}{6881280}e^{10} \\ k_1 = -\frac{1}{8}e^2 + \frac{1}{96}e^4 + \frac{3840}{49}e^6 + \frac{322560}{2251}e^8 + \frac{14971}{5160960}e^{10} \\ k_2 = \frac{13}{384}e^4 + \frac{17}{2560}e^6 - \frac{19423}{3440640}e^8 - \frac{250811}{41287680}e^{10} \\ k_3 = -\frac{61}{3840}e^6 - \frac{899}{107520}e^8 + \frac{823}{286720}e^{10} \\ k_4 = \frac{49561}{5160960}e^8 + \frac{175087}{20643840}e^{10} \\ k_5 = -\frac{34729}{5160960}e^{10} \end{cases}$	$\begin{cases} k_0 = -\frac{1}{4}e^2 + \frac{17}{192}e^4 + \frac{9}{1280}e^6 + \frac{26581}{5160960}e^8 + \frac{19937}{6881280}e^{10} \\ k_1 = -\frac{1}{2}n + \frac{7}{6}n^2 - \frac{27}{20}n^3 + \frac{697}{1260}n^4 - \frac{5}{1008}n^5 \\ k_2 = \frac{13}{24}n^2 - \frac{209}{120}n^3 + \frac{3821}{2688}n^4 + \frac{19771}{5760}n^5 \\ k_3 = -\frac{61}{120}n^3 + \frac{1663}{2688}n^4 - \frac{1081}{840}n^5 \\ k_4 = \frac{49561}{20160}n^4 - \frac{420}{20160}n^5 \\ k_5 = -\frac{34729}{5040}n^5 \end{cases}$

On the basis of Equation (6), the inverse solution formula of the Gauss-Krüger projection complex variable function represented by “double Angle form” is derived as follows:

$$\theta = -\omega + \sin 2\omega(l_1 + (l_2 + (l_3 + (l_4 + l_5 \cos 2\omega) \cos 2\omega) \cos 2\omega) \cos 2\omega) \quad (15)$$

According to Equation (6), the coefficients in Equation (15) are:

$$\begin{cases} l_1 = b_2 - b_6 + b_{10} \\ l_2 = 2b_4 - 4b_8 \\ l_3 = 4b_6 - 12b_{10} \\ l_4 = 8b_8 \\ l_5 = 16b_{10} \end{cases} \quad (16)$$

Similarly, the coefficients in Equation (15) are expanded in terms of  $e$  up to  $e^{10}$  and in terms of  $n$  up to  $n^5$ , which is shown in Table 7:

**Table 7.** Coefficients in Equation (15).

Coefficient Representation Based on $e$	Coefficient Representation Based on $n$
$\begin{cases} l_1 = -\frac{1}{8}e^2 - \frac{1}{48}e^4 - \frac{43}{1920}e^6 + \frac{121}{161280}e^8 + \frac{2189}{1720320}e^{10} \\ l_2 = \frac{1}{384}e^4 + \frac{1}{640}e^6 + \frac{35701}{10321920}e^8 + \frac{4211}{5160960}e^{10} \\ l_3 = -\frac{17}{7680}e^6 - \frac{283}{107520}e^8 - \frac{25373}{13762560}e^{10} \\ l_4 = -\frac{4397}{5160960}e^8 + \frac{1319}{860160}e^{10} \\ l_5 = -\frac{4583}{10321920}e^{10} \end{cases}$	$\begin{cases} l_1 = -\frac{1}{2}n + \frac{2n^2}{3} - \frac{8n^3}{5} + \frac{4699n^4}{630} - \frac{131881n^5}{5040} \\ l_2 = \frac{n^2}{24} + \frac{2n^3}{15} - \frac{4015n^4}{8064} - \frac{1969n^5}{2520} \\ l_3 = -\frac{17n^3}{120} + \frac{37n^4}{210} + \frac{1013n^5}{1920} \\ l_4 = -\frac{4397n^4}{20160} + \frac{4177n^5}{1260} \\ l_5 = -\frac{4583n^5}{10080} \end{cases}$

To sum up, based on the theory of complex functions, three kinds of complex function expressions of the Gauss-Krüger projection are derived by the computer algebraic system. These expressions are completely equivalent, and all are symbolic expressions that are suitable for any reference ellipsoid.

**4. Truncation Difference Analysis**

According to the series expansion principle, the larger the expansion order is, the higher the corresponding precision is, and the longer the corresponding expression is. The derived expansions of Equations (4), (6), (9), (11), (13) and (15) are symbolic expressions applicable to the earth ellipsoid of any parameter. In this paper, the CGCS2000 national geodetic coordinate system is taken as an example to carry out numerical analysis on the three forms of complex function expressions of the Gauss-Krüger projection and analyze their truncation difference when expanded to different orders. Ellipsoid parameters of CGCS2000: Major axis:  $a = 6378137$  m; Flatness:  $f = 1/298.257222101$ ; The first eccentricity:  $e = 0.0818191910428152$  [29].

The basic idea of the analysis is as follows: select a Gauss-Krüger projection band  $P = \{(B, l) : |l| \leq 3^\circ, 60^\circ \leq B \leq 90^\circ\}$ , calculate the projection coordinate  $(x_0, y_0)$  through the traditional real number formula given in [15,27], calculate the coordinate value  $(x_i, y_i)$  through the forward solution expansion Formula (4) of “multiple Angle form”, and calculate the difference, respectively, to get the calculation difference of the forward projection solution. The difference distribution is shown in Figures 4 and 5:

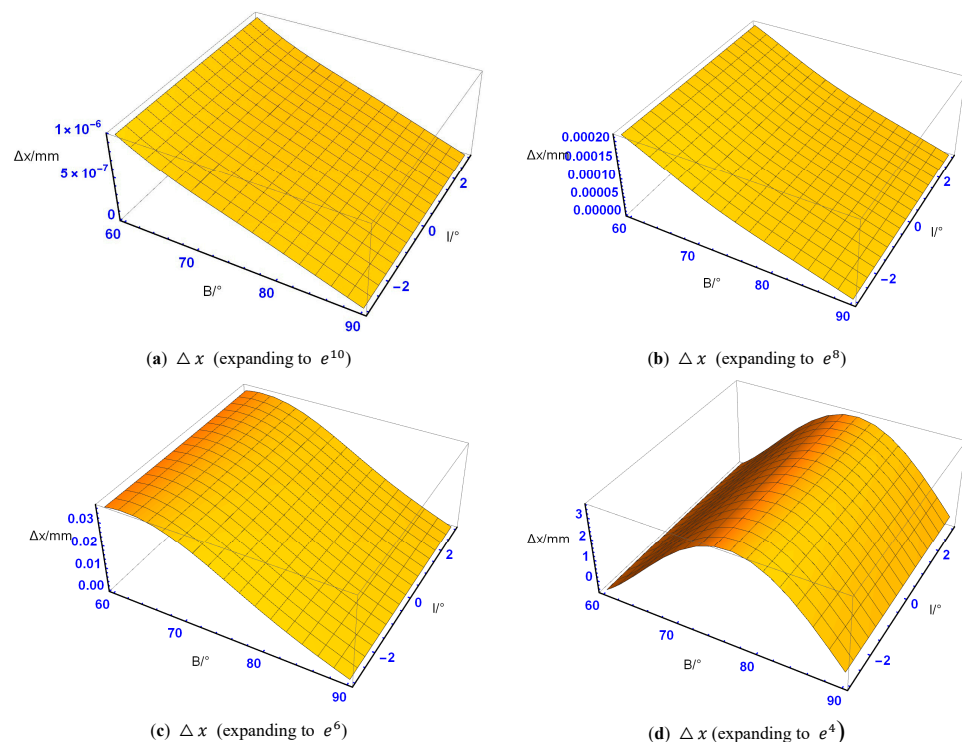


**Figure 4.** The distribution of the abscissa truncation difference  $\Delta x$  when expanding to  $e^{10}$ ,  $e^8$ ,  $e^6$ , and  $e^4$ .

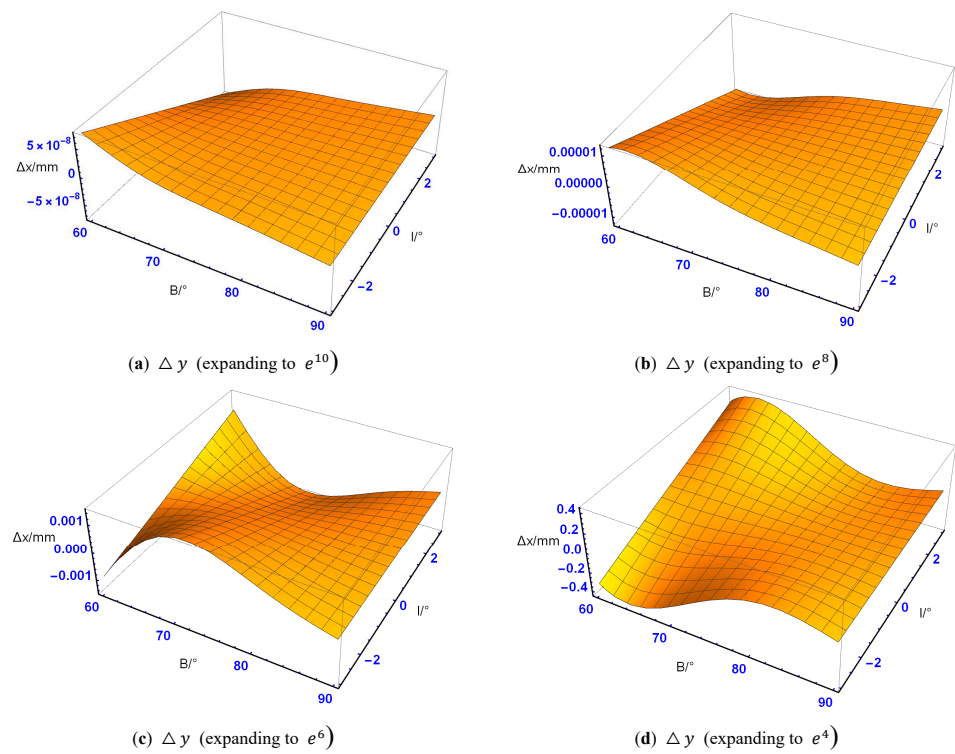


**Figure 5.** The distribution of the ordinate truncation difference  $\Delta y$  when expanding to  $e^{10}$ ,  $e^8$ ,  $e^6$ , and  $e^4$ .

Similarly, selecting the Gauss-Krüger projection band  $P = \{(B, l) : |l| \leq 3^\circ, 60^\circ \leq B \leq 90^\circ\}$ , the difference distribution of the expansion of the forward solution in the form of multiple angles based on the expansion of the third flattening  $n$  is shown in Figures 6 and 7:

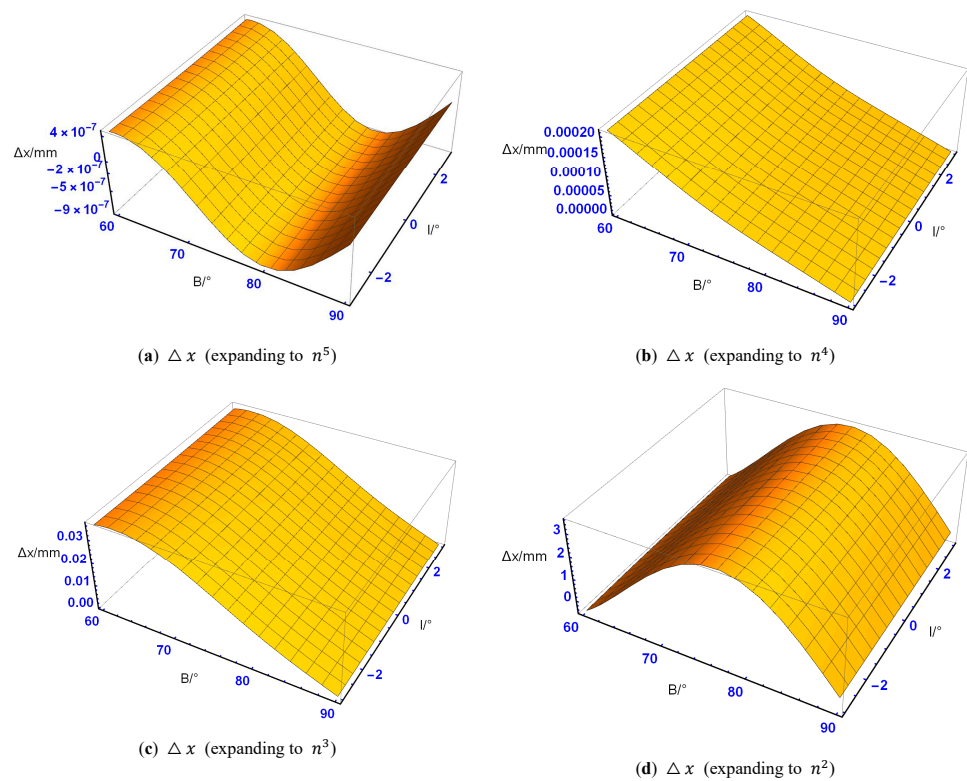


**Figure 6.** The distribution of the abscissa truncation difference  $\Delta x$  when expanding to  $n^5$ ,  $n^4$ ,  $n^3$ , and  $n^2$ .

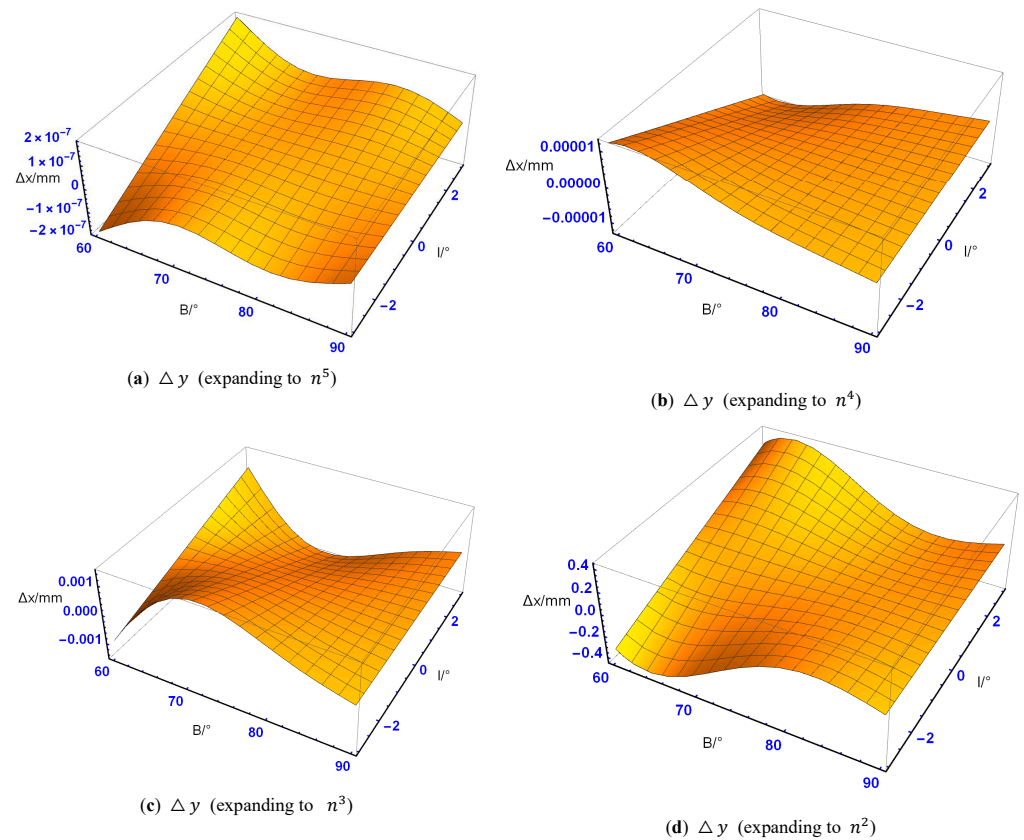


**Figure 7.** The distribution of the ordinate truncation difference  $\Delta y$  when expanding to  $n^5$ ,  $n^4$ ,  $n^3$ , and  $n^2$ .

Similarly, selecting a Gauss-Krüger projection band  $Q = \{(x, y) : 0 \text{ km} \leq x \leq 6600 \text{ km}, |y| \leq 500 \text{ km}\}$ , the ellipsoid coordinate  $(B_0, l_0)$  is calculated by the inverse solution formula given in [26], then the coordinate  $(B_i, l_i)$  is calculated by the inverse solution expansion Formula (6) in the “multiple Angle form”, and the calculation difference  $(\Delta B, \Delta l)$  of the inverse solution is obtained by calculating the difference, respectively. The difference distribution is shown in Figures 8 and 9:

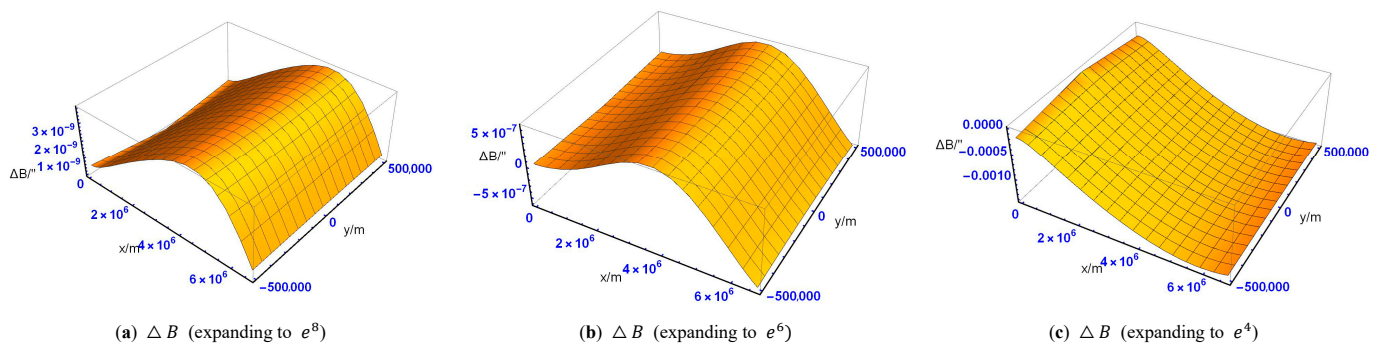


**Figure 8.** The distribution of the latitude truncation difference  $\Delta B$  when expanding to  $e^8$ ,  $e^6$ , and  $e^4$ .

Similarly, based on the expansion of the third flattening  $n$ , the difference distribution of the expansion of the inverse solution of the “multiple Angle form” is shown in Figures 10 and 11:

As can be seen from Figures 4–11, when the forward and inverse complex function expressions of the Gauss-Krüger projection are expanded to the same order based on the ellipsoid eccentricity  $e$  and the third flattening  $n$ , the calculation differences are not much different, which can be regarded as equal precision. When the expression of the

forward solution is expanded to  $e^{10}$  and  $n^5$ , the coordinate calculation differences ( $\Delta x$ ,  $\Delta y$ ) are of the order of  $10^{-7}$  mm. When the inverse solution expression is expanded to  $e^{10}$  and  $n^5$ , the order of coordinate calculation difference ( $\Delta x$ ,  $\Delta y$ ) is  $10^{-9}$ ". The truncation difference of the forward and inverse solution can meet the requirements of geodesy well, but the corresponding power series expansion formulas are also a little long and complicated. According to [26], the calculation accuracy of the expansion is related to the expansion order. When the expressions are expanded to  $e^6$  and  $n^3$ , the order of magnitude of calculation difference ( $\Delta x$ ,  $\Delta y$ ) of the forward solution is  $10^{-2}$  mm, and the order of magnitude of calculation difference ( $\Delta B$ ,  $\Delta l$ ) of the reverse solution is  $10^{-4}$ ", both of which meet the accuracy requirements. In addition, the expressions are more concise and practical.

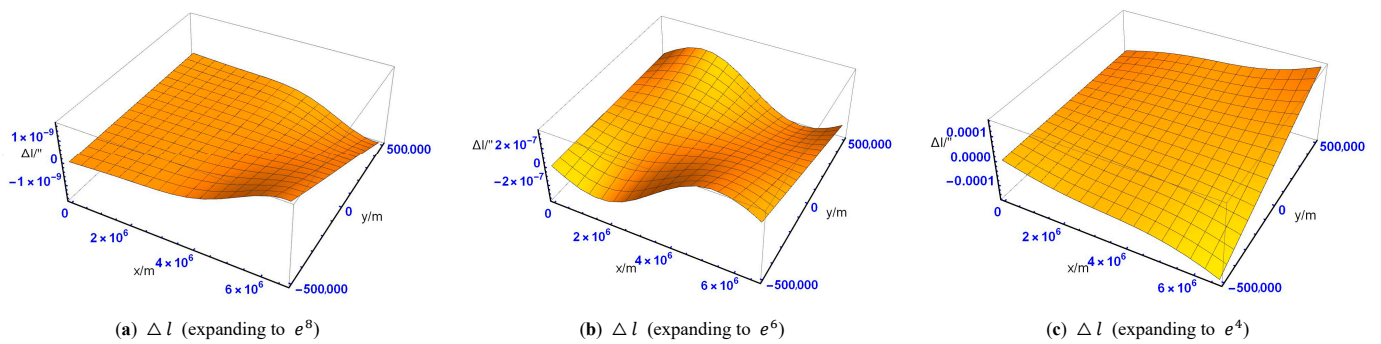


Figure 9. The distribution of the longitude truncation difference  $\Delta l$  when expanding to  $e^8$ ,  $e^6$ , and  $e^4$ .

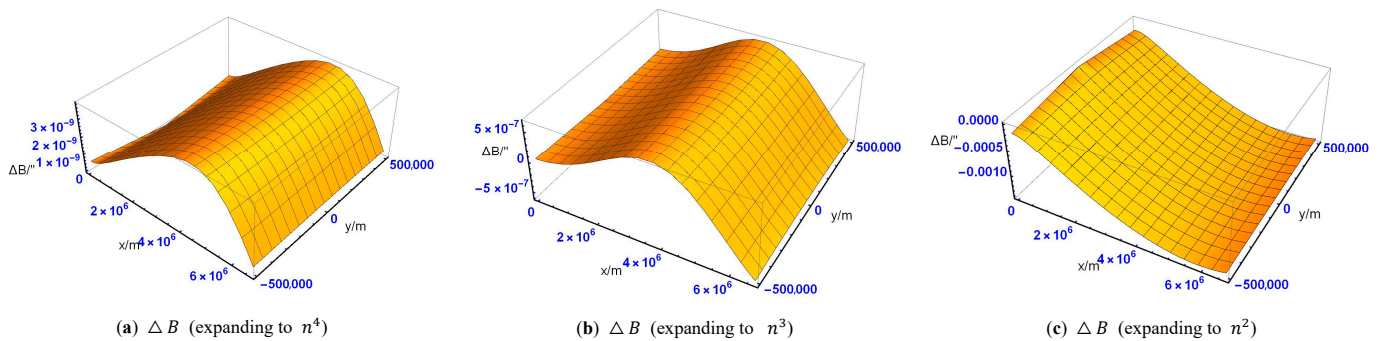


Figure 10. The distribution of the latitude truncation difference  $\Delta B$  when expanding to  $n^4$ ,  $n^3$ , and  $n^2$ .

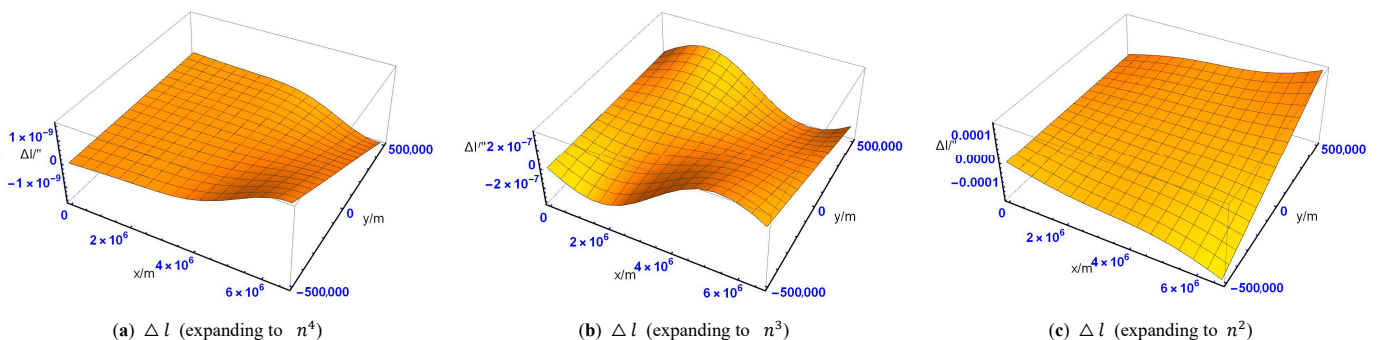
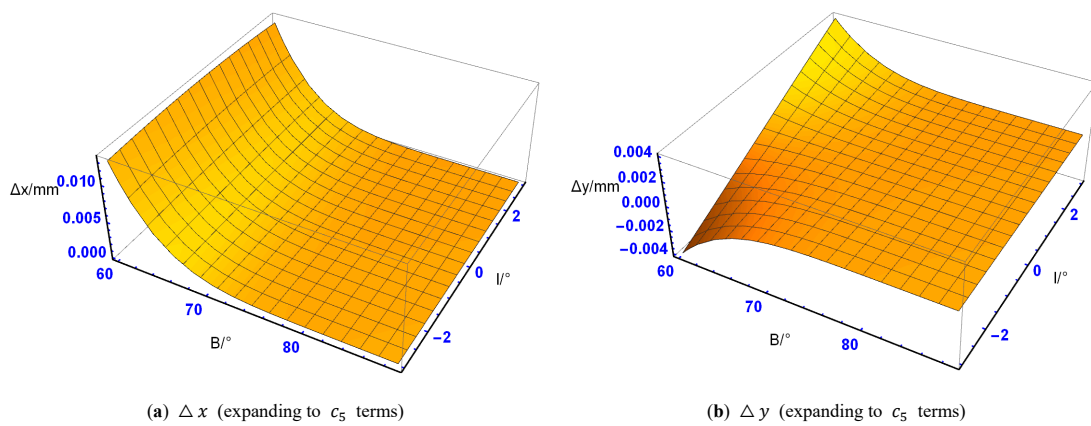
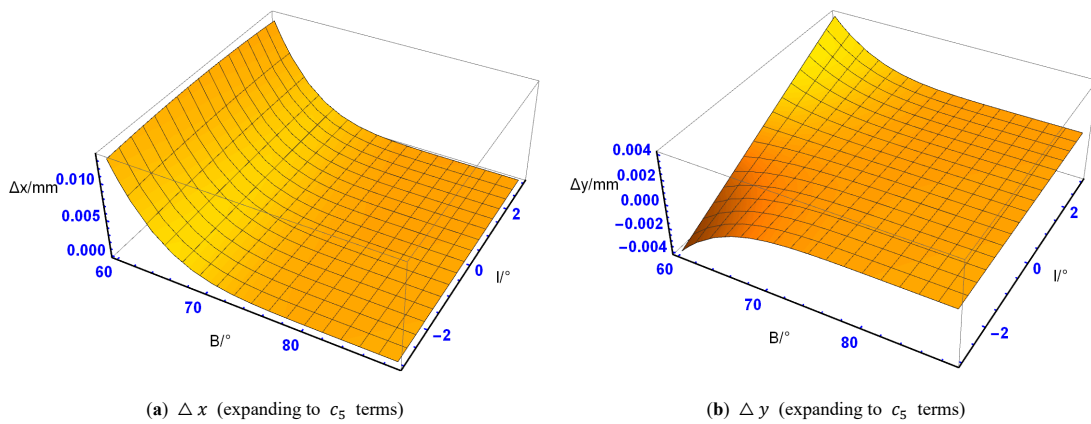


Figure 11. The distribution of the longitude truncation difference  $\Delta l$  when expanding to  $n^4$ ,  $n^3$ , and  $n^2$ .

Similarly, for the forward solution expression (9) in “power exponential form”, by analyzing the truncation differences of the expression expanded to different terms, it can be concluded that when the expression is expanded to  $c_5$ , the order of magnitude of calculation difference ( $\Delta x$ ,  $\Delta y$ ) of the forward solution is  $10^{-3}$  mm. The distribution of ( $\Delta x$ ,  $\Delta y$ ) is shown in Figures 12 and 13:



**Figure 12.** The distribution of  $(\Delta x, \Delta y)$  when expanding to  $c_5$  terms (based on  $e$ ).



**Figure 13.** The distribution of  $(\Delta x, \Delta y)$  when expanding to  $c_5$  terms (based on  $a$ ).

For the inverse solution expression (11) in the form of “power exponent”, by analyzing the truncation difference of the expansion to different terms, it can be concluded that the order of magnitude of calculation difference of the inverse solution when the expression is expanded to  $j_5$  terms is  $10^{-6}$ . The variation trend of the latitude and longitude calculation difference  $(\Delta B, \Delta l)$  is shown in Figures 14 and 15:

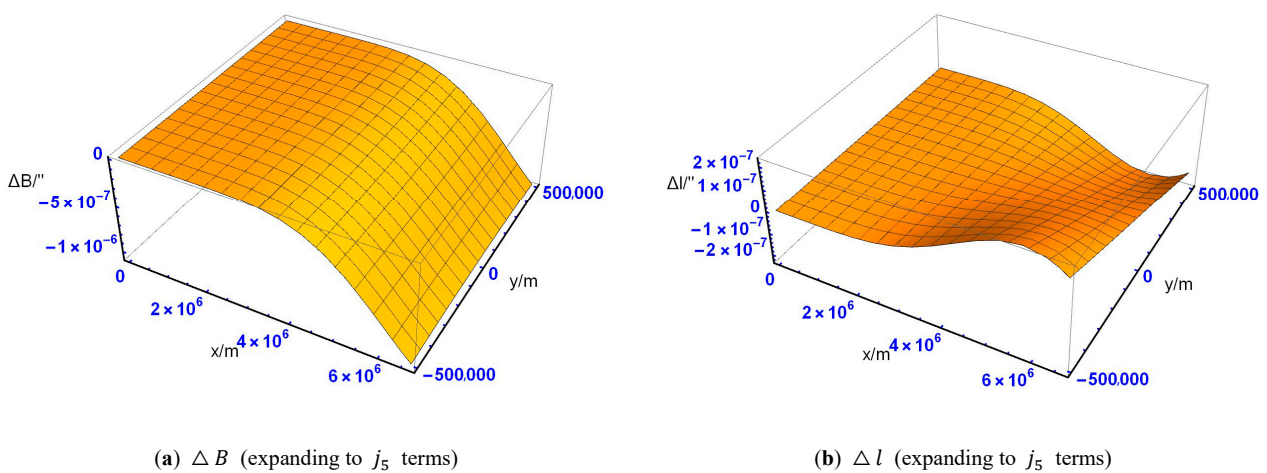


**Figure 14.** The distribution of  $(\Delta B, \Delta l)$  when expanding to  $j_5$  terms (based on  $e$ ).

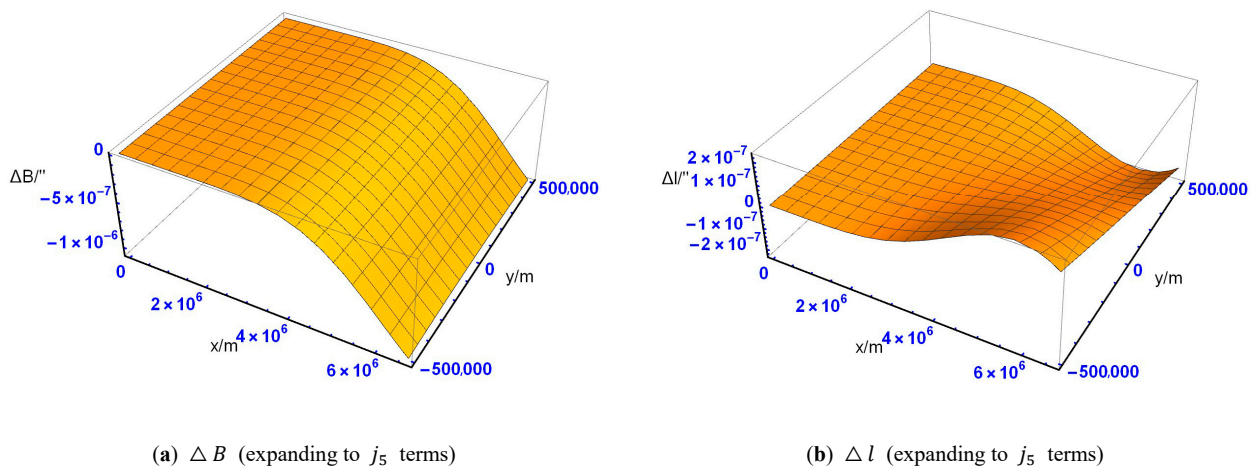


Figure 15. The distribution of  $(\Delta B, \Delta l)$  when expanding to  $j_5$  terms (based on  $n$ ).

For the forward solution expression (13) in the form of “double Angle form”, by analyzing the truncation difference of the expression expanded to different terms, it can be concluded that the order of magnitude of the forward solution calculation difference is  $10^{-2}$  mm when the expression expanded to  $k_3$  terms, and the variation trend of the coordinate calculation difference  $(\Delta x, \Delta y)$  is shown in Figures 16 and 17:

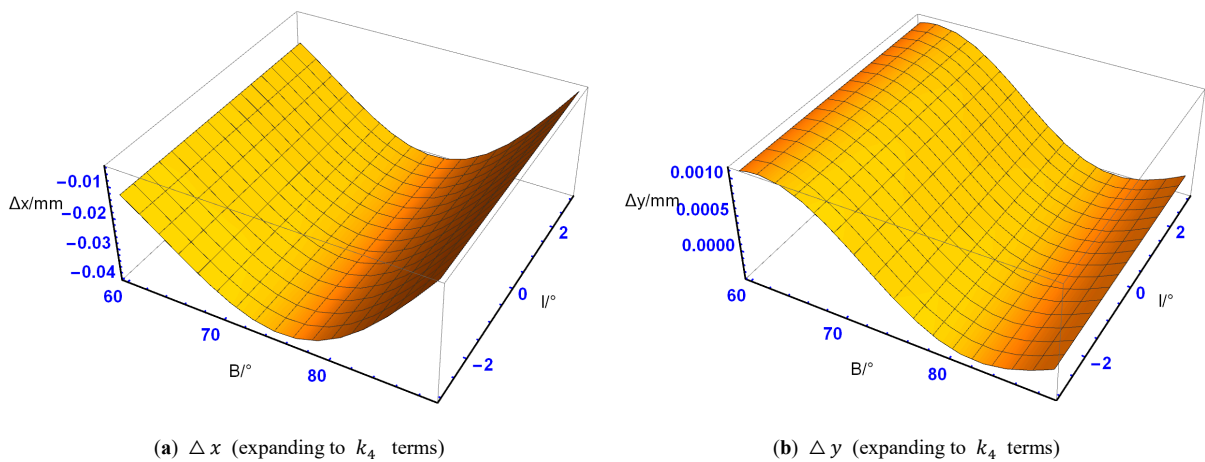


Figure 16. The distribution of  $(\Delta x, \Delta y)$  when expanding to  $k_3$  terms (based on  $e$ ).

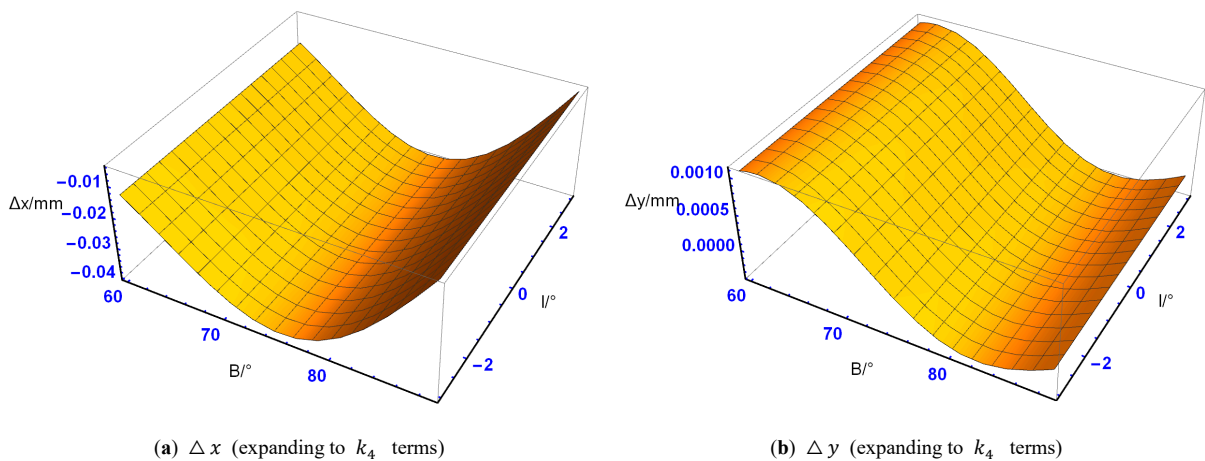


Figure 17. The distribution of  $(\Delta x, \Delta y)$  when expanding to  $k_3$  terms (based on  $n$ ).

For the inverse solution expression (15) in the form of “double Angle form”, by analyzing the truncation difference of the expansion to different terms, it can be concluded that the order of magnitude of calculation difference of inverse solution when the expression is expanded to  $l_3$  terms is  $10^{-7}''$ , and the variation trend of latitude and longitude calculation difference ( $\Delta B$ ,  $\Delta l$ ) is shown in Figures 18 and 19:

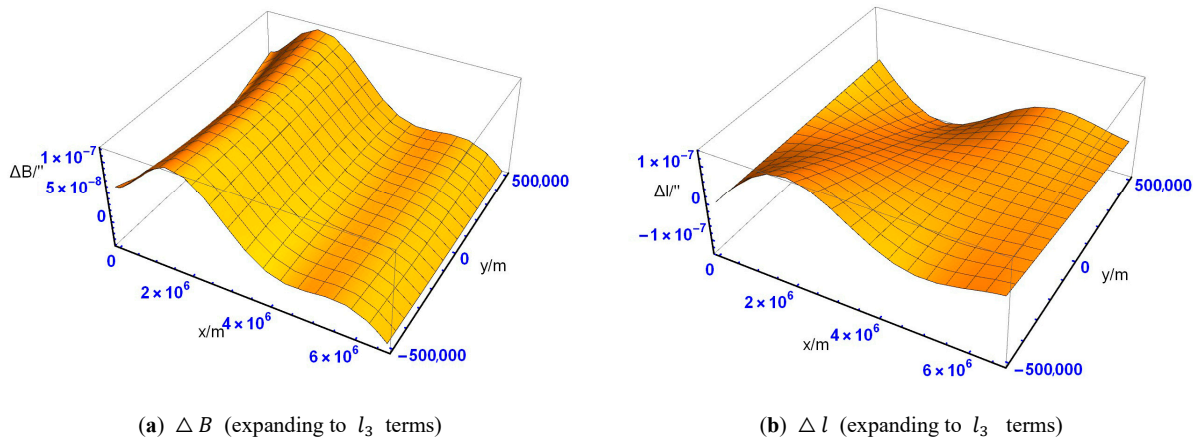


Figure 18. The distribution of ( $\Delta B$ ,  $\Delta l$ ) when expanding to  $l_3$  terms (based on  $e$ ).

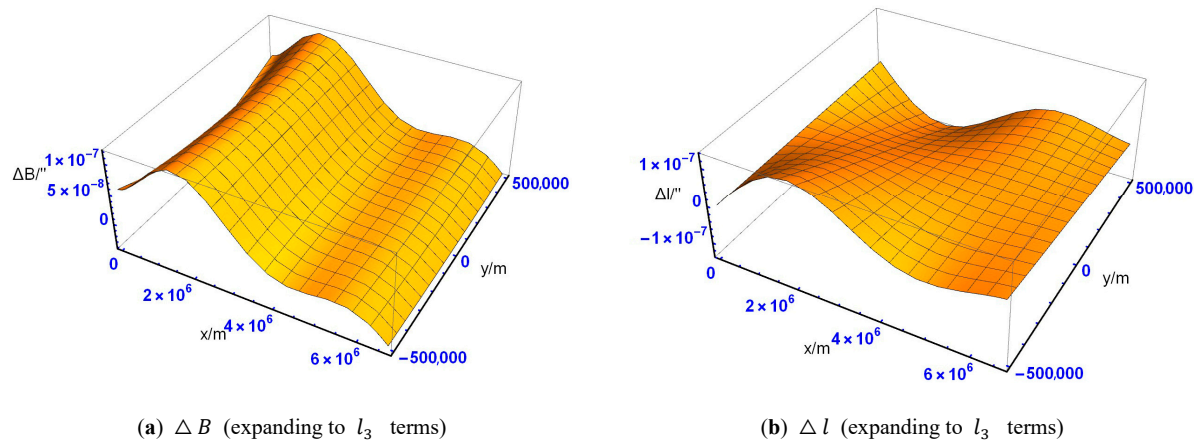


Figure 19. The distribution of ( $\Delta B$ ,  $\Delta l$ ) when expanding to  $l_3$  terms (based on  $n$ ).

To sum up, on the premise of meeting the accuracy requirements of geodesy, the simplified expressions of the complex functions of the three forms of the Gauss-Krüger projection are as follows:

The expression in “multiple Angle form”:

$$z = x + iy \approx a(\alpha_0\theta - \alpha_2 \sin 2\theta + \alpha_4 \sin 4\theta - \alpha_6 \sin 6\theta) \tag{17}$$

$$\theta \approx -\omega + b_2 \sin 2\omega + b_4 \sin 4\omega + b_6 \sin 6\omega \tag{18}$$

The expression in “exponential form”:

$$z = x + iy \approx ac_0\theta + a \cos \theta (c_1 \sin \theta + c_3 \sin^3 \theta + c_5 \sin^5 \theta) \tag{19}$$

$$\theta \approx -\omega + (j_1 \sin \omega + j_3 \sin^3 \omega + j_5 \sin^5 \omega) \cos \omega \tag{20}$$

The expression in “double Angle form”:

$$z = x + iy \approx ak_0\theta + a \sin 2\theta (k_1 + (k_2 + k_3 \cos 2\theta) \cos 2\theta) \tag{21}$$

$$\theta \approx -\omega + \sin 2\omega(l_1 + (l_2 + l_3 \cos 2\omega) \cos 2\omega) \quad (22)$$

### 5. Case Analysis and Calculation Efficiency Analysis

Through the above derivation, three forms of simplified expressions (17–22) for complex functions of the Gauss-Krüger projection are obtained that meet the accuracy requirements. In order to verify their efficiency, the CGCS2000 ellipsoid constant is selected for an example analysis. Take the region  $0^\circ \leq B \leq 90^\circ$ ,  $-3^\circ \leq l \leq 3^\circ$  ( $0 \text{ km} \leq x \leq 6000 \text{ km}$ ,  $-500 \text{ km} \leq y \leq 500 \text{ km}$ ) that contains the poles, where the number of points can be determined by the resolution of geodetic latitude and longitude directions. Take the resolution of  $1' \times 1'$  ( $2 \text{ km} \times 2 \text{ km}$ ) as an example, including  $5401 \times 217$  ( $3001 \times 501$ ) points.

Taking the above region as an example, the computational efficiency of all formulas in the paper is analyzed. Through the traditional formula of real numbers (Formula (1)), the forward solution takes  $T_f$  and the inverse solution takes  $T_i$ .

Through the “multiple Angle form” formula, when expanding to  $a_{10}$  terms, it takes  $T_{1f}$  for the forward solution (Formula (4)); and when expanding to  $b_{10}$  terms, it takes  $T_{1i}$  for the inverse solution (Formula (6)). When expanding to  $a_6$ , it takes  $t_{1f}$  for the forward solution (Formula (17)); and when expand to  $b_6$ , it takes  $t_{1i}$  for the inverse solution (Formula (18)).

Through the “exponential form” formula, when expanding it to  $c_9$  terms, it takes  $T_{2f}$  for the forward solution (Formula (9)); and when expanding to  $j_9$  terms, it takes  $T_{2i}$  for the inverse solution (Formula (11)). When expanding to  $c_5$ , it takes  $t_{2f}$  for the forward solution (Formula (19)); and when expanding to  $j_5$ , it takes  $t_{2i}$  for the inverse solution (Formula (20)).

Through the “double Angle form” formula, when expanding it to  $k_5$  terms, it takes  $T_{3f}$  for the forward solution (Formula (13)); and when expanding to  $l_5$  terms, it takes  $T_{3i}$  for the inverse solution (Formula (15)). When expanding to  $k_3$ , it takes  $t_{3f}$  for the forward solution (Formula (21)); and when expand to  $l_3$ , it takes  $t_{3i}$  for the inverse solution (Formula (22)).

The derived algorithm is compiled and run on a 2.90 GHz Intel processor by software Matlab2017a. The calculation results are shown in Table 8:

**Table 8.** Calculation time of different formulas (unit: s).

Forward solutions	Group	$T_f$	$T_{1f}$	$t_{1f}$	$T_{2f}$	$t_{2f}$	$T_{3f}$	$t_{3f}$
	Time		4281	5.714	4.471	6.738	5.127	5.132
Inverse solutions	Group	$T_i$	$T_{1i}$	$t_{1i}$	$T_{2i}$	$t_{2i}$	$T_{3i}$	$t_3$
	Time		37.21	7.938	6.711	9.083	7.434	7.421

According to Table 8, because of the integration and iteration operation involved, the calculation efficiency is very low when using the traditional real formula. When complex functions are introduced and series expansion is adopted, the new forward and inverse solution formulas only involve the sum and multiplication of trigonometric functions, which greatly improves the computational efficiency. By comparing  $T_{1f}$ ,  $T_{2f}$ , and  $T_{3f}$ , it can be found that the calculation efficiency of the form of “double Angle” is highest, which is close to that of the form of “multiple Angle”, while the calculation efficiency of the form of “exponential” is the lowest. By comparing  $t_{1f}$ ,  $t_{2f}$ , and  $t_{3f}$ , it can be found that the calculation efficiency of the three forms of inverse solution formulas also has a similar rule. By comparing  $T_{1f}$  and  $t_{1f}$ , it can be found that the lower-order terms are more efficient for both forward and inverse solutions. In conclusion, after precision analysis, truncation difference analysis, and calculation efficiency analysis, the Gauss-Krüger projection complex function expression in the “double Angle form” not only meets the requirements of geodesy, but also improves the calculation efficiency relatively well when expanded to  $k_3$  terms; especially for the case of higher resolution and more points, the superiority of the improved formula is more prominent, and it can better meet the requirements of modern electronic charts for higher map resolution and more efficient projection transformation.

## 6. Summary

In this paper, the mathematical mapping relation between ellipsoid coordinates and map plane coordinates is solved based on the theory of complex functions. With the help of the computer algebra system Mathematica, the improved complex function expressions of the Gauss-Krüger projection are derived in three forms. The formulas derived are symbolic expressions and are applicable to any reference ellipsoid. Moreover, each formula is expanded in a power series based on  $e$  and  $n$ , respectively. Taking CGCS2000 reference ellipsoid as an example, the numerical analysis is carried out. By analyzing the truncation difference when the expression is expanded to different orders, the simpler expansion formula satisfying the requirement of geodetic precision is obtained, which improves the calculation efficiency to a certain extent and makes the formula easier to use and spread. Furthermore, taking  $5401 \times 217$  ( $3001 \times 501$ ) points as an example, by comparing the time it takes to calculate the forward and inverse coordinate solutions with different formulas, it is verified that the complex function expression of the Gauss-Krüger projection of the “double Angle form” is the least time-consuming and the highest computational efficiency. To sum up, this paper starts from the mathematical basis of map projection theory, the complicated and lengthy higher-order expansions are abandoned, and we improve the efficiency of projection transformation by improving the coordinate transformation formula on the premise of ensuring the accuracy of projection transformation.

**Author Contributions:** Conceptualization, Xiaoyong Li and Houpu Li; Formal analysis, Xiaoyong Li and Shaofeng Bian; Funding acquisition, Houpu Li; Investigation, Xiaoyong Li and Guohui Liu; Methodology, Xiaoyong Li, Houpu Li, Guohui Liu and Shaofeng Bian; Resources, Xiaoyong Li and Shaofeng Bian; Software, Guohui Liu; Supervision, Shaofeng Bian; Validation, Guohui Liu and Houpu Li; Visualization, Xiaoyong Li and Shaofeng Bian; Writing—original draft, Xiaoyong Li; Writing—review & editing, Shaofeng Bian and Houpu Li. All authors have read and agreed to the published version of the manuscript.

**Funding:** This work was supported by The National Science Foundation for Outstanding Young Scholars of China (42122025); The National Natural Science Foundation of China (41971416, 41876222).

**Data Availability Statement:** All data generated or analysed during this study are included in this published article.

**Acknowledgments:** The earth parameters in this paper are CGCS2000, which are public data. Mathematica and Matlab were used for image presentation and data analysis. We express our sincere gratitude to these organizations and software providers.

**Conflicts of Interest:** The authors declare no conflict of interest.

## References

1. Grafarend, E.; You, R.; Syffus, R. *Map Projections*; Springer: Berlin/Heidelberg, Germany, 2014.
2. Lapaine, M.; Usery, E.L. *Map Projection Definition*; Springer: Berlin/Heidelberg, Germany, 2017; Chapter 9; pp. 213–228. [CrossRef]
3. Skopeliti, A.; Tsoulos, L. Choosing a Suitable Projection for Navigation in the Arctic. *Mar. Geod.* **2013**, *36*, 234–259. [CrossRef]
4. Bugayevskiy, L.; Snyder, J. *Map Projections: A Reference Manual*; Taylor and Francis: London, UK, 1995.
5. Deng, X.; Tang, Z.; Hua, X.; Shu, Y. Gauss-Krüger Projection Forward and Reverse Calculation of after Ellipsoid Transformation. *J. Geod. Geodyn.* **2010**, *30*, 49–52.
6. Bildirici, I.O. Numerical inverse transformation for map projections. *Comput. Geosci.* **2003**, *29*, 1003–1011. [CrossRef]
7. Guo, Y.; Chen, H.; Zhang, X. Realization of Accurate Conversion Algorithm between Google Earth UTM Coordinates and Geodetic Coordinates. *Surv. Mapp. Geol. Miner. Resour.* **2012**, *28*, 10–13.
8. Zhuang, P. Gauss-Krüger Projection Calculation. *Surv. Mapp. Geol. Miner. Resour.* **1998**, 24–27.
9. Deakin, R.E.; Hunter, M.N.; Karney, C. The Gauss-Krüger Projection. 2010. Available online: [https://www.academia.edu/354352/The\\_Gauss\\_Krueger\\_Projection](https://www.academia.edu/354352/The_Gauss_Krueger_Projection) (accessed on 4 November 2022).
10. Abbey, D.; Woolhouse, L.; Featherstone, W. The Oblique Mercator for engineering and survey. *Surv. Rev.* **2022**, 1–12. [CrossRef]
11. Baselga, S. Two Conformal Projections for Constant-Height Surface to Plane Mapping. *J. Surv. Eng.* **2021**, *147*, 06020004. [CrossRef]
12. Bian, S.; Li, H.; Li, Z. Research Progress in Mathematical Analysis of Map Projection by Computer Algebra. *Acta Geod. Cartogr. Sin.* **2017**, *46*, 1557–1569.
13. Clenshaw, C.W. A note on the summation of Chebyshev series. *Math. Comput.* **1955**, *9*, 118–120. [CrossRef]

14. Ablowitz, M.J.; Fokas, A.S. *Complex Variables: Applications of Complex Function Theory*; Cambridge University Press: Cambridge, UK, 2003.
15. Bowring, B. The Transverse Mercator Projection—A Solution by Complex Numbers. *Surv. Rev.* **1978**, *30*, 325–342. [[CrossRef](#)]
16. Klotz, J. Eine Analytische Lösung der Gauss-Krueger-Abbildung. *Z. Für Vermess.* **1993**, *118*, 106–115.
17. Schuhr, P. Transformationen zwischen ellipsoidischen geographischen Konformen Gauss-Krueger bzw UTM-Koordinaten. *Forum* **1995**, *5*, 259–264.
18. Bian, S.; Zhang, C. Complex function representation of Gauss projection. *J. Inst. Surv. Mapp.* **2001**, *18*, 157–159.
19. Li, H.; Bian, S. The Expressions of Gauss Projection by Complex Numbers. *Acta Geod. Cartogr. Sin.* **2008**, *37*, 5–9.
20. Liu, Q.; Bian, S.; Li, Z. Closed formulae of Gauss Projection with Its Deformation on Sphere. *J. Nav. Univ. Eng.* **2015**, *27*, 45–49. (In Chinese)
21. Guo, J.; Shen, W.; Ning, J. Development of Lee's exact method for Gauss-Krüger projection. *J. Geod.* **2020**, *94*, 1–16. [[CrossRef](#)]
22. Lee, L. Conformal Projections Based On Jacobian Elliptic Functions. *Int. J. Geogr. Inf. Geovisualization* **1976**, *13*, 67–101. [[CrossRef](#)]
23. Karney, C. Transverse Mercator with an accuracy of a few nanometers. *J. Geod.* **2011**, *85*, 475–485. [[CrossRef](#)]
24. Bermejo-Solera, M.; Otero, J. Simple and highly accurate formulas for the computation of Transverse Mercator coordinates from longitude and isometric latitude. *J. Geod.* **2009**, *83*, 1–12. [[CrossRef](#)]
25. Yang, Q.; Snyder, J.; Tobler, W. *Map Projection Transformation: Principles and Applications*; CRC Press: Boca Raton, FL, USA, 2020.
26. Xiong, J. *Ellipsoid Geodesy*; Chinese People's Liberation Army Publishing House: Beijing, China, 1988.
27. Bian, S.; Zhang, C. The Gauss Projection-A Solution by Complex Numbers. *J. Inst. Surv. Mapp.* **2001**, *18*, 157–159.
28. Li, X.; Li, H.; Liu, G.; Bian, S.; Jiao, C. Simplified Expansions of Common Latitudes with Geodetic Latitude and Geocentric Latitude as Variables. *Appl. Sci.* **2022**, *12*, 7818. [[CrossRef](#)]
29. Peng, X.; Gao, J.; Wang, J. Research of the Coordinate Conversion between WGS84 and CGCS2000. *J. Geod. Geodyn.* **2015**, *35*, 219–221.